STRAIN-INDUCED TRANSFORMATION TOUGHENING IN METASTABLE AUSTENITIC STEELS

R.G. Stringfellow* and D.M. Parks*

The phenomenon by which metastable austenitic steels transform into a harder martensite phase accompanied by plastic deformation is termed "strain-induced transformation plasticity" (SITP). Certain high strength alloys of this type have displayed remarkably high fracture toughness, which can be attributed to the transformation process and its effect on the fracture event. We propose a constitutive model for SITP. Careful consideration is given to four critical features of the transformation process: transformation hardening, transformation shape-strain, transformation dilatation, and the stress-state sensitivity of the transformation kinetics. We implement the constitutive model numerically and examine the effect of the transformation on the state of stress and strain near the tip of a stationary crack.

INTRODUCTION

Under suitable thermodynamic conditions, γ-austenite, a metastable phase with an FCC structure, undergoes a phase transformation into α'-martensite, with a much harder BCC or BCT structure. Within a certain temperature range, with a lower bound referred to as M_s^σ and an upper bound referred to as M_d, the transformation occurs only in the presence of an applied stress which exceeds the yield strength of the austenite. In this temperature range, the transformation process is governed by slip in the parent austenite. Specifically, the intersection of micro-shear bands in the austenite is thought to generate new nucleation sites for martensitic embryos (Olson and Cohen (1)). This phenomenon has been given the name *strain-induced transformation plasticity.*

Experiments conducted on a 31Ni-5Cr high strength (tensile yield stress = 1300 MPa) precipitation-hardened austenite stainless steel that displays this unique property have produced extremely high values for fracture toughness, J_{Ic} = 300 MPa–m (Leal (2)). Data from recent experiments suggest that still higher toughness values ($J_{Ic} \sim$ 590 MPa–m) are achievable at this strength level (Stavehaug (3)). In light of the inverse relationship between strength and toughness that is generally observed, this combination of strength and toughness is remarkable.

*Department of Mechanical Engineering, Massachusetts Institute of Technology, Cambridge, MA 02139

CONSTITUTIVE MODEL

The kinetics of the transformation process are functions of temperature and plastic strain, and are sensitive to the local state of stress (Young (4); Olson et al (5)). Considering the very high levels of triaxiality found near the tip of a crack, this feature of the transformation process is thought to be critical for the understanding of the observed toughness enhancement in SITP steels. The one-dimensional model developed by Olson and Cohen (1) for the formation of martensite in the strain-induced regime has been extended to include the effects of the stress state and cast in a rate form. The model is based on the assumption that nucleation occurs predominantly at shear-band intersections. The rate of increase in the volume fraction of martensite, $\dot{f}$, is postulated to be proportional to the rate of increase in the number of martensitic embryos per unit austenite volume, $\dot{N}^{\alpha'}$:

$$\dot{f} = (1 - f)\, \bar{v}^{\alpha'} \dot{N}^{\alpha'} , \tag{1}$$

where $\bar{v}^{\alpha'}$ is the average volume per martensitic unit, which is assumed to be constant. $N^{\alpha'}$ is assumed to be equal to the number of shear-band intersections per unit volume, $N^I = \hat{N}^I(\Theta, \gamma_a)$, multiplied by the transformation probability, $P = \hat{P}(\Theta, \Sigma)$, where Θ represents a normalized temperature, γ_a is the plastic shear strain in the austenite, and Σ is a measure of the "triaxiality" of the state of stress ($\Sigma = -p/\sqrt{3}\bar{\tau}$, where p is pressure and $\bar{\tau}$ is equivalent shear stress). Details of the model development are given in Stringfellow et al (6). Under isothermal conditions, $\dot{f}$ can be expressed as:

$$\dot{f} = A_f \dot{\gamma}_a + B_f \dot{\Sigma} , \tag{2}$$

where A_f and B_f depend upon $P(\Theta, \Sigma)$ and $\dot{\gamma}_a$. The probability parameter, P, is cast in the form of a cumulative probability distribution function,

$$P = \frac{1}{\sqrt{2\pi}} \int_{-\infty}^{x} exp\left[-\frac{1}{2} \left(\frac{x' - \bar{x}}{s_x} \right)^2 \right] dx' , \tag{3}$$

where $\bar{x}$ is the dimensionless mean of a given probability distribution function and s_x is its standard deviation. The parameter x is defined to be:

$$x = x_0 - x_1 \Theta + x_2 \Sigma , \tag{4}$$

where x_0, x_1 and x_2 are dimensionless constants.

The variable x is a critical parameter for determining the extent of transformation under different conditions. It can be viewed as a measure of the normalized chemical driving force for transformation: x decreases with increasing temperature but increases with increasing triaxiality.

We compared our model predictions with data taken from Young (4), who measured the extent of martensite evolution with plastic strain during both simple tension and simple compression tests on a 10Ni-16Cr-0.5Mn-0.33P-0.25C phospho-carbide strengthened SITP alloy. The results of his tests are shown in Fig. 1 along with a fit to the data using our model.

A hypoelastic formulation is used to define the evolution of the stress state as a function of the rate kinematics. The evolution equation for the average stress in the composite, $\mathbf{T}$, is given by:

$$\overset{\nabla}{\mathbf{T}} = \mathcal{L}^e [\mathbf{D} - \mathbf{D}^p] , \tag{5}$$

where $\overset{\nabla}{\mathbf{T}}$ is the Jaumann stress rate tensor, and the stretching tensor, $\mathbf{D}$, has been decomposed into its elastic and plastic parts: $\mathbf{D} = \mathbf{D}^e + \mathbf{D}^p$. We assume that $\mathcal{L}^e = \mathcal{L}^e_a = \mathcal{L}^e_m$.

We introduce the following further decomposition of the plastic stretching rate tensor: $\mathbf{D}^p = \mathbf{D}^{slip} + \mathbf{D}^{nucl}$, where $\mathbf{D}^{slip}$ is the part of the plastic stretching which is due to slip and $\mathbf{D}^{nucl}$ is an additional strain rate which is a result of the transformation process. We propose the following form for $\mathbf{D}^{nucl}$:

$$\mathbf{D}^{nucl} = \dot{f}\left(A\mathbf{N} + \frac{1}{3}\triangle_V \mathbf{1}\right) , \tag{6}$$

where A is constant, $\mathbf{N}$ is the unit tensor coaxial with the stress deviator, $\triangle_V$ is the transformation volume change and $\mathbf{1}$ is the second order identity tensor.

We further define $\mathbf{D}^{slip} = 1/\sqrt{2}\dot{\bar{\gamma}}\mathbf{N}$, where $\dot{\bar{\gamma}}$ is the average equivalent plastic shear slip rate of the evolving two-phase composite. Of critical importance is the apportioning of the strain rates in the individual phases. Previous models for strain-induced transformation plasticity have been based on the Voigt model. Because of the high hardness differences between the austenite and martensite, Voigt predictions lead to overestimates of the composite stress. We therefore utilize a self-consistent estimate of the strain-rate decomposition, which has been outlined in Stringfellow and Parks (7).

The assumption of material isotropy leads to the separation of (5) into two scalar equations for the evolution of the stress invariants. A solution of these two equations in conjunction with evolution equations for f, and the hardnesses of the austenite and martensite phases, s_a and s_m, provides a complete description of the constitutive model for SITP steels.

MODEL IMPLEMENTATION and ANALYSIS

The model has been implemented as a material-law subroutine which can be incorporated into the finite element code ABAQUS.

To illustrate the importance of the stress-state sensitivity of the transformation, we first consider a very simple one-element model under five states of stress, each characterized by a different level of triaxiality. The results are summarized in Fig 2. The evolution of martensite with equivalent plastic strain, shown at the bottom of Fig 2, indicates dramatic differences between the extreme cases of plane-strain tension versus plane-strain compression. These data suggest that at higher triaxialities, such as near a crack tip, where $\Sigma > 2.0$, significant amounts of martensite can form even at temperatures that are well above the M_d temperature for uniaxial tension. Fig 3 shows how dramatically the martensite changes the stress-strain curve. Note the early strain-softening for the plane-strain tension case, This is a result of the transformation strain-rate term which was incorporated into the model.

We then consider the blunting of an initially sharp crack undergoing mode I loading. The analysis is patterned after McMeeking (8). A schematic of the boundary value problem is shown in Fig 3. The domain of the problem is a fan-shaped area which represents a region surrounding the tip of a crack that is well within the confines of any physical boundaries, such that the body can be considered to be infinite in extent, as shown in Fig 3(a) The Mode I load is applied by imposing the linear elastic, asymptotic crack-tip (K_I) displacement field along the outer boundary of the model.

Two cases are considered: One case with a non-transforming, power-law hardening material, representing 100% austenite, and one case where the model temperature is such that transformation occurs only in regions where the triaxiality is substantially greater than that of uniaxial tension.

RESULTS and DISCUSSION

Fig 4(a) shows the extent of transformation near the tip of the blunted crack. Due to the triaxial nature of the stress-state ahead of the crack tip, a considerable amount of martensite forms in this region. Because the strain decays rapidly ahead of the crack tip, the extent of the transformed region is limited; the peak level of martensite thus occurs well before the point at which peak triaxiality is found, as illustrated in Fig 4(b).

Fig 5 compares contours of composite hardness in the crack tip region for the transforming and non-transforming cases. Due to the evolution of the much harder martensite phase, an area of increased hardness is formed directly ahead of the crack tip.

Significant differences between the non-transforming and transforming cases were found for the parameter $h/\bar{\sigma}$, where $h = \triangle\bar{\sigma}/\triangle\epsilon$ is the (incremental) hardening rate. In uniaxial tension, the onset of necking occurs when $h/\bar{\sigma} = 1$, and plastic flow is unstable for values of $h \leq \bar{\sigma}$. In this sense, $h/\bar{\sigma}$ can be thought of as a flow stability parameter, lending qualitative insight into the tendency for plastic flow to localize (Needleman and Rice (9)). For standard power-law hardening materials, stability becomes more and more difficult to maintain as the strain increases. In steels which undergo SITP, however, the dramatic strain-hardening caused by the transformation process delays the final loss of stability to much higher strain levels.

For the crack problem, the effect of the unique shape of the stress-strain curve is profound. In Fig 6 we have plotted contours of $h/\bar{\sigma}$ for the transforming and non-transforming cases. In the non-transforming case, "stability" is lost at all points where $\epsilon > 0.10$. In the transforming case, the loss of stability is limited to a very short region in front of the crack, and there is a region (whose shape resembles the shape of the martensite zone) in which the plastic flow is stable, due to the strain-hardening influence of the martensite.

In the absence of transformation, high strength steels generally fail by a process of shear instability resulting in the classical "zig-zag" pattern of crack propagation (Van den Avyle(10)). In light of the observed fracture mechanisms and the previously described flow stablizing effects of the transformation, it seems likely that transformation hardening delocalizes the deformation and retards this process.

The high strain *and* high triaxiality levels found ahead of the crack tip lead to formation of a zone of hard martensite in which plastic flow is stable. The forward zig-zag pattern of crack propagation by localization into shear bands is prevented by this stable zone. On the other hand, on the crack flanks above and below the crack tip are regions with relatively little transformation and hardening, but with a high *rate* of transformation, and thus a high rate of strain softening. The tendency toward localization will thus be great in these regions, and it is quite likely that shear bands will form here.

Recent experiments by Stavehaug (3) support this notion. For non-transforming materials, he observed the classical zig-zag pattern of crack propagation. For transforming materials, however, he observed that the crack often

branched, leading to significant blunting of the crack prior to further advance of one of the branches. The deflection of the crack front away from the forward direction appears to be a major factor contributing to the observed high toughnesses.

REFERENCES

(1) Olson, G. and Cohen, M., *Met. Trans.* Vol. 6A, 1975, pp. 791-5.

(2) Leal, R., Ph.D. Thesis, MIT, Cambridge, MA, USA, 1984.

(3) Stavehaug, F., Ph.D. Thesis, MIT, Cambridge, MA, USA, 1990.

(4) Young, C.–C., Ph.D. Thesis, MIT, Cambridge, MA, USA, 1988.

(5) Olson, G., Tsuzaki, K. and Cohen, M., *Mat. Res. Soc. Symp. Proc*, Vol. 57, 1987, pp. 129-148.

(6) Stringfellow, R., Parks, D. and Olson, G., manuscript in prep.

(7) Stringfellow, R. and Parks, D., to appear in *Int. J. Plast.*

(8) McMeeking, R., *J. Mech. Phys. Solids*, Vol. 25, 1977, pp. 357-381.

(9) Needleman, A. and Rice, J., in *Mechanics of Sheet Metal Forming*, Koistinen, and Wang, eds., Plenum, New York, 1978, pp. 237-65.

(10) Van den Avyle, J., Ph.D. Thesis, MIT, Cambridge, MA, USA, 1975.

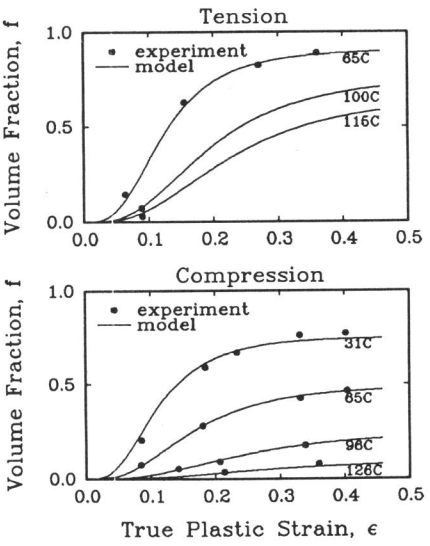

Fig 1 Comparison of model predictions with data of Young (4).

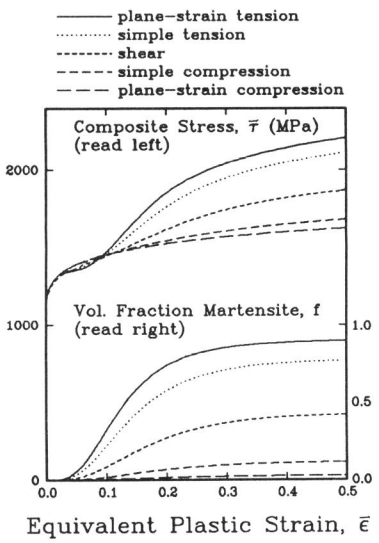

Fig 2 One element test results. Model data taken from Young (4).

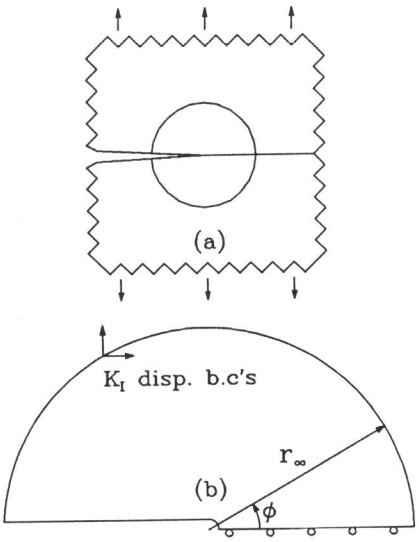

Fig 3 Schematic of model for crack blunting analysis.

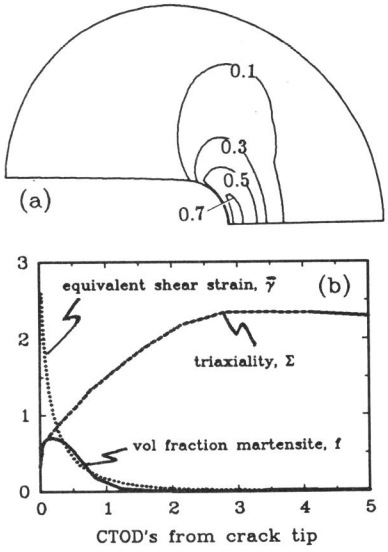

Fig 4 (a) Contours of f. (b) values of f, Σ, and $\bar{\gamma}$ ahead of the crack tip.

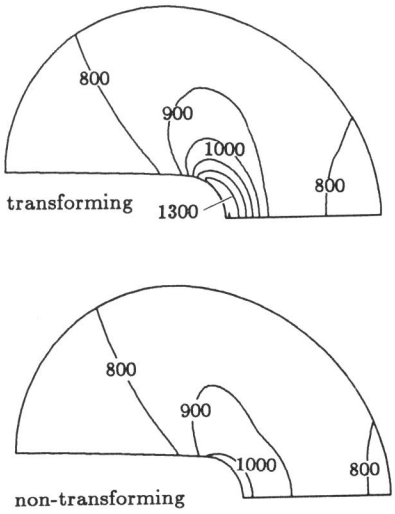

Fig 5 Contours of equivalent shear stress, $\bar{\tau}$ (MPa).

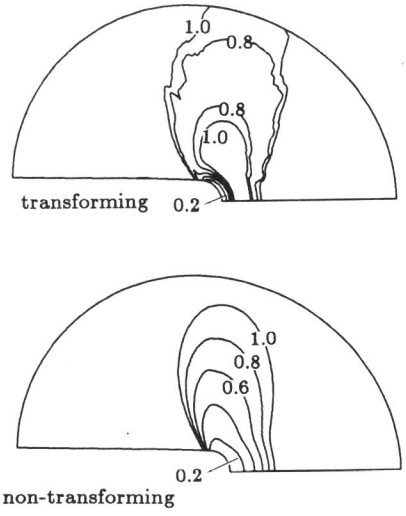

Fig 6 Contours of the stability parameter, $h/\bar{\sigma}$.